

See discussions, stats, and author profiles for this publication at: <https://www.researchgate.net/publication/229109089>

# Improved statistical methods applied to surface chemistry in minerals flotation

ARTICLE *in* MINERALS ENGINEERING · MAY 2006

Impact Factor: 1.6 · DOI: 10.1016/j.mineng.2005.09.039

---

CITATIONS

25

---

READS

13

3 AUTHORS, INCLUDING:



**Brian R. Hart**

The University of Western Ontario

45 PUBLICATIONS 489 CITATIONS

SEE PROFILE



**Mark C. Biesinger**

The University of Western Ontario

51 PUBLICATIONS 2,470 CITATIONS

SEE PROFILE

# Improved statistical methods applied to surface chemistry in minerals flotation

Brian Hart<sup>a</sup>, Mark Biesinger<sup>a</sup>, Roger St.C. Smart<sup>b,\*</sup>

<sup>a</sup> Surface Science Western, University of Western Ontario, London, Ont., Canada N6A 5B7

<sup>b</sup> Applied Centre for Structural and Synchrotron Studies (ACeSSS), University of South Australia, Building H2-18, Mawson Lakes Campus, Adelaide, South Australia 5095, Australia

Received 28 June 2005; accepted 9 September 2005

Available online 25 October 2005

## Abstract

Diagnosis of the surface chemical factors playing a part in flotation separation of a value sulfide phase requires measurement of the hydrophobic and hydrophilic species that are statistically different between the concentrate and tail streams. Statistical methods, based on the monolayer-sensitive time of flight secondary ion mass spectrometry (ToF-SIMS) technique, have been developed towards this ultimate aim by measuring hydrophobic species (collector ions, dimers and metal complexes, polysulfides) as well as hydrophobic metal ions, precipitates and added depressant species. Reliable identification of specific mineral particles is central to this statistical analysis. A chalcopyrite/pyrite/sphalerite mineral mixture conditioned at pH9 for 20 min to study transfer of Cu from chalcopyrite via solution to the other two mineral surfaces, since this mechanism can be responsible for their inadvertent flotation in copper recovery, showed no statistical difference in the copper intensities on pyrite and sphalerite (selected from Fe and Zn images) after this conditioning. Principal component analysis (PCA) identifies combinations of factors strongly correlated (positively or negatively) in images or spectra from sets of data. In images, PCA selects these correlations from the mass spectra recorded at each of  $256 \times 256$  pixels in a selected area of particles. In the image mode, PCA has proved to be a much better method of selecting particles by mineral phase with clearer definition of particle boundaries due to multi-variable recognition. It has clearly separated a statistical difference in copper intensities between the sphalerite and pyrite phases.

The PCA method has been applied to concentrate and tails samples collected from the Inco Matte Concentrator demonstrating extensive CuOH and NiOH transfer between the chalcocite (Cc) and heazlewoodite (Hz) minerals. Statistical differences illustrate the important discriminating depressant action of NiOH in flotation despite the activation of Hz by Cu transfer. The adsorption of the collector at specifically-identified Cu sites has been elucidated by the study. Importantly, the statistical analysis has been able to confirm some mechanisms and deny others proposed to control recovery and selectivity giving more focus on the control factors.

© 2005 Elsevier Ltd. All rights reserved.

**Keywords:** Mineral flotation; Surface chemistry; ToF-SIMS; Principal component analysis

## 1. Introduction

In the selective separation of mineral phases by flotation, surface chemistry is the principal determinant of the average contact angle for a specific mineral phase in a flotation pulp. The average contact angle is, in turn, the

principal determinant of the bubble-particle attachment efficiency ( $E_a$ ) in the overall collection efficiency ( $E_c$ ) from which the flotation rate constant can be determined (Ralston, 1994). The recovery and selectivity in sulfide flotation is ultimately dependent on the relative rate constants of the different mineral phases. But the average contact angle is not only mineral-specific, based on a statistical average of the mineral particles in that phase, but also the contact angle for each particle is an average of hydrophobic and hydrophilic areas across the particle surface. Determination

\* Corresponding author. Tel.: +61 8 83023353; fax: +61 8 83023799.  
E-mail address: [roger.smart@unisa.edu.au](mailto:roger.smart@unisa.edu.au) (R.St.C. Smart).

of this hydrophobic/hydrophilic balance by particle therefore requires selection of the particular mineral phase and statistical analysis of the particles with an estimation of the spread of values. In a flotation pulp containing many different mineral phases, different particle sizes of individual phases, adsorbed and precipitated species (often colloidal), and oxidised products, this is not a simple task.

The hydrophobic/hydrophilic balance by particle and its statistical average by mineral phase requires identification of the major species contributing to each category in surface layers (Smart et al., 2003a). In addition to adsorbed collector molecules and their oxidised products (e.g. dimers), hydrophobicity can be imparted to sulfide mineral surfaces by oxidation to produce polysulfide  $S_n^{2-}$  species resulting from loss of metal ions (usually  $Fe^{2+}$ ) from surface layers. In acid solution, hydrophobic elemental sulfur can also be formed usually imaged in patches on the sulfide mineral surface (Smart et al., 2003b). Almost all other species found on sulfide mineral surfaces, such as oxide/oxyhydroxide/hydroxides, oxy-sulfur (e.g. sulfate), carbonate, hydrous silica and fine gangue particles, are essentially hydrophilic but may be in the form of localised particles, colloids and precipitates or continuous, reacted or precipitated surface layers (Smart et al., 2003b).

The action of collector molecules in inducing hydrophobicity can be assisted by activating species such as copper and lead ions that complex the collector on the surface. Previous research has shown that this activation can be inadvertently produced by dissolution and transfer via solution of these ions to mineral phases not intended to float (Smart, 1991; Lascelles and Finch, 2002; Finkelstein, 1997). The mechanisms of activation of sphalerite (Gerson et al., 1999) and pyrite (Weisener and Gerson, 2000) by copper have been elucidated. In this paper, we first examine statistical evidence for this mechanism on both mixed mineral (chalcopyrite/pyrite/sphalerite) samples. The 1–2 monolayer-sensitive time of flight secondary ion mass spectrometry (ToF-SIMS) technique has been used in our previous work (e.g. Piantadosi et al., 2000) to develop a statistical method for comparing surface species between particles of the same mineral phase in feed, concentrate and tail streams. The mineral particles are normally identified by imaging for a major element of their composition, e.g. Cu, Fe or Zn, but this selection can be difficult with many multi-metal minerals (e.g. chalcopyrite) and with precipitated, adsorbed, reacted and contaminant species in the outermost molecular layers. Hence, a challenge in the work is to find more reliable methods of mineral phase recognition in these complex surface chemistries. We will show that principal component analysis (PCA) provides this improvement in phase recognition and particle selection.

The second case examines solution transfer of activating copper ions and depressant nickel ions in a plant study from the Inco Sudbury Matte Concentrator. The PCA analysis identifies the controlling surface chemical mechanisms including collector action. We have been able to extend the PCA analysis to directly compare statistical

weightings for surface species between concentrate and tails without the need for particle selection. This method offers major reduction in data processing time and moves the methodology closer to routine diagnostic application.

Some of this work has been reported previously at the Fifth UBC–McGill Biennial International Symposium on Fundamentals of Mineral Processing, August 2004 (Biesinger et al., 2004) and the Centenary of Flotation Symposium (Hart et al., 2005).

## 2. Experimental

### 2.1. Sample preparation and mounting

The chalcopyrite/pyrite/sphalerite mixed mineral sample was conditioned with a pH 9 solution of sodium hydroxide for 20 min. The chalcocite/heazlewoodite plant samples were collected from the Inco Matte Concentrator plant (C. Valenius) following the sampling methodology, developed and tested previously (Smart, 1991), to remove dissolved oxygen, snap-freeze to stop reaction. They were received in a frozen state, were thawed then washed three times in a pH 12 solution of sodium hydroxide. Each slurry sample was pressed into indium foil and transferred to the introduction chamber of the ToF-SIMS with the mineral surfaces still wet, i.e. without contact with air. The remaining liquid is then pumped away in the vacuum.

### 2.2. ToF-SIMS surface analysis

The ToF-SIMS technique, used in static mode, involves a very low flux of heavy ions (in this case,  $Ga^+$ ) impacting surface layers with mass spectrometric analysis of the secondary ions emitted from the surface. In the time of routine measurement, only 1–2 surface atoms in 1000 are impacted. The secondary elemental and molecular fragment ions come from the first two molecular layers of the surface and provide a very detailed set of positive and negative mass fragments from simple ions, e.g.  $Na^+$ ,  $OH^-$  through to molecular ions of specific reagents, e.g. isobutyl xanthate  $(CH_3)_2CHOCS_2^-$ . Identification of molecular mass peaks for collectors, activators, depressants, precipitates and adsorbed species is possible with comparative surface concentrations by particle and by phase between feed, concentrate and tail streams. In the method developed at the Ian Wark Research Institute, a lateral distribution imaging of species by particle is combined with a statistical comparison of differences between streams by mineral phase (Piantadosi et al., 2000).

### 2.3. Single specie ion image mineral phase identification

Individual phase recognition in a multi mineral mixture was originally accomplished by scanning for regions of high ion yield peculiar to a selected mineral phase. Specific ion images were normalized to the total ion yield removing topographic and/or matrix effects in an attempt to clearly define the phase associated with the selected ion (Fig. 1).

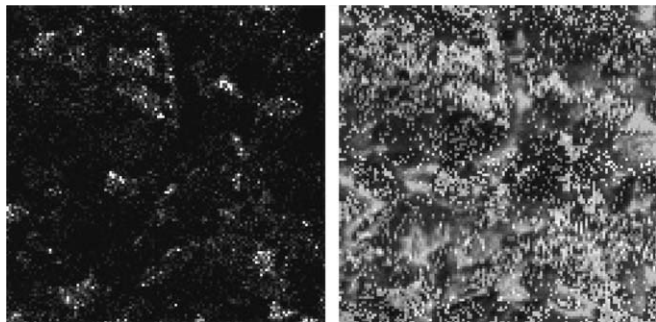


Fig. 1. ToF-SIMS positive ion images of particles in the pyrite/sphalerite/chalcopyrite mixture. Left: Zn ion distribution (raw). Right: Zn ion distribution after normalization to the total ion image. Zn ROIs representing a specific mineral phase appear bright in both images. Images are  $100 \times 100 \mu\text{m}$ .

Regions of interest (ROI) were then mapped and mass spectra collected for 30 ROIs representing each mineral phase. Statistical analyses were performed on phase specific spectra after normalization to total ion yield and area.

#### 2.4. Principal component analysis (PCA)

Consider a  $256 \times 256$  pixel ToF-SIMS image data set obtained over a mass range of 1000 amu containing over  $6.5 \times 10^7$  data points or variables. With such a large data set, extracting and analyzing the relevant data, in this case, mineral phases, becomes a major issue. Fortunately, the variables are usually correlated such that the most important information is contained in a smaller number of components. Principal component analysis is employed to determine these components.

Related to a ToF-SIMS imaging data matrix ( $X$ ), each sample point ( $m$ ), or pixel in the image, will have  $n$  variables (mass spectral intensities) associated with it. The data matrix  $X$  is organized into  $m$  rows and  $n$  columns. Calculation of the PCA model decomposes the data matrix  $X$  into submatrices represented in Fig. 2 and by the following equation:

$$X = t_1 p_1^T + t_2 p_2^T + \dots + t_k p_k^T + \dots + t_q p_q^T \quad (1)$$

where  $t_i$  are the scores (images),  $p_i$  are the loadings (mass spectral intensities),  $q \leq \min\{m, n\}$ , and the  $t_i p_i$  pairs are ordered by the amount of variance captured. The first principal component will account for as much of the variability in the data as possible, and each succeeding component will account for as much of the remaining variability as possible. In ToF-SIMS data, this first principal component is often

associated with large topographic and matrix variations in the data (ion yield variations across the sample) (Biesinger et al., 2002). Successive components will describe the various chemical components in order of importance; in this case, mineral phases and other materials (gangue, mounting materials) within the imaged data set. These components will be relatively free of topographic and matrix effects.

Generally the model is truncated, leaving some small amount of variance in a residual matrix ( $E$ ) giving the following equation:

$$X = t_1 p_1^T + t_2 p_2^T + \dots + t_k p_k^T + E = T_k P_k^T + E \quad (2)$$

The PCA model is calculated using the following equations:

$$\text{cov}(X) = (X^T X) / (m - 1) \quad (3)$$

$$\text{cov}(X) = \lambda_i p_i \quad (4)$$

where  $\text{cov}(X)$  is the covariance matrix of  $X$ ,  $X^T$  is the transpose of  $X$  and  $\lambda_i$  are the eigenvalues. The amount of variance captured by  $t_i p_i$  is proportional to  $\lambda_i$ . The resulting scores and loadings can then be examined and related to chemistry of the sample being explored. Typically, the majority of the variability within a system can be described in a relatively low number of principal components (scores and loading sets) allowing for an accelerated investigation of the data set. PCA is a well-established technique and a full description of it can be found elsewhere (Mardia et al., 1979; Massart et al., 1997).

#### 2.5. PCA software

PLS\_Toolbox 2.1 from Eigenvector Research Ltd. (Manson, WA, USA) running on Matlab 6.0 was the software used for PCA analysis. For each set of data as many significant mass peaks as possible were added to the peak list for analysis. Also included in the peak selection is the total remaining ion image (sum of ion intensity not selected as a specific peak) shown at mass zero in the loadings. Data was either “mean centred” or “autoscaled” prior to PCA. Mean centring is done by subtracting the column mean from each column, thus forming a matrix where each column has a mean of zero. For the “autoscaled” data, the data is first mean centred and each mean centred variable is then divided by its standard deviation resulting in variables with unit variance. This procedure puts all variables on an equal basis in the analysis. Thus, the less intense but more chemically significant higher mass peaks receive the same level of consideration in the analysis as the intense, low mass peaks.

### 3. Results and discussion

#### 3.1. Mixed mineral system

ToF-SIMS statistical analysis is reported for a chalcopyrite/pyrite/sphalerite mineral mixture conditioned at pH 9

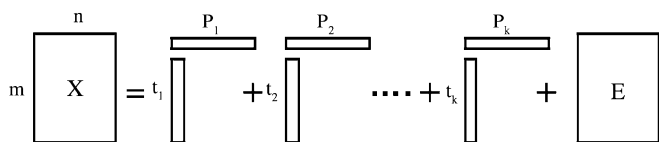


Fig. 2. A schematic representation of the principles of principal component analysis.



for 20 min in order to study transfer of Cu from chalcopyrite via solution to the other two mineral surfaces. This mechanism can be responsible for their inadvertent flotation in copper recovery. In particular, preferential adsorption of copper ions between pyrite and sphalerite was examined. The system provided an opportunity to compare the results from the single specie ion image mineral phase identification to the PCA differentiation method and, to test the reliability of the latter.

The difficulty of phase recognition can be appreciated from Fig. 3 where the range of particle sizes is illustrated. Initially, phase recognition of pyrite and sphalerite was based on single specie ion (i.e. Fe, Zn respectively) image mineral phase identification as outlined above. Results after mineral phase differentiation, ROI mass spectra collection and processing for Fe, Zn and Cu are given in Fig. 4. The data indicate that pyrite differentiation is accomplished by mapping the Fe distribution even with the presence of Fe (bulk and surface) in sphalerite. Differentiation of sphalerite based on Zn distribution however is complicated by Zn on pyrite which results in some uncertainty as to species recognition. The Cu analyses by phase also suggests that there is no statistical difference between the copper adsorbed on pyrite and sphalerite, contrary to most studies which indicate a preference for adsorption on sphalerite but without direct evidence (Smart, 1991; Lascelles and Finch, 2002; Finkelstein, 1997). The lack of Cu selectivity is not related to mineral surface chemistry but to the poor differentiation between pyrite and sphalerite grains (see Fig. 4).

In an alternative statistical analysis, principal component analysis (PCA) was used to enhance phase recognition and definition of regions for mass spectral analysis. This is the first application of PCA to flotation surface chemistry. (Biesinger et al., 2004). In images, PCA selects correlations from the mass spectra recorded at each of  $256 \times 256$  pixels ( $6.5 \times 10^7$  data points) in a selected area of particles. Fig. 5 shows the image scores and factor loadings for the “auto-

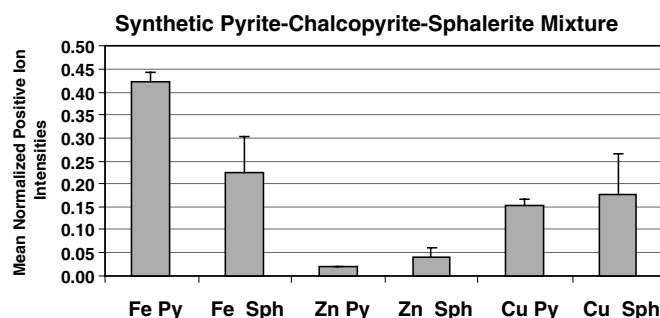


Fig. 4. Statistical phase identification from single specie ion image identification and copper distribution between pyrite and sphalerite. Line bars are 95% confidence intervals.

scaled” positive ion image data set (four significant principal components). The first principal component, labeled PC1, shows factor loadings that are positive in weighting for all masses. This component is representative of the largest variance in the data set; topography and matrix (ion yield intensity) fluctuations. The second and subsequent PC’s will then have this variance removed and as such are topography- and matrix-corrected.

PC2 shows positive weightings for zinc mass peaks and negative weighting for iron and copper mass peaks. Thus, bright areas on the image score are indicative of zinc rich (sphalerite) phases. The dark areas are thus rich in iron and copper; however, separation of pyrite and chalcopyrite phases is not yet accomplished.

As separation of pyrite and chalcopyrite had not been shown, a second PC analysis was carried out using “mean centred” data (Fig. 6). Using mean centred data will place more emphasis in the principal component analysis on stronger ion images (such as iron and copper). PC1 again produces factor loadings and images representative of the largest variance in the data set; topography and matrix (ion yield intensity) fluctuations and is usefully removed from subsequent PCs. PC2 in Fig. 6 shows a strong

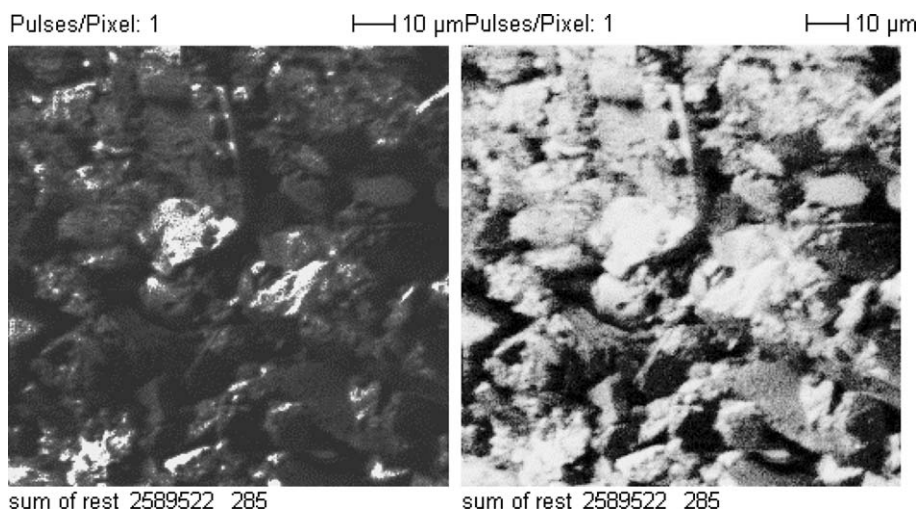


Fig. 3. ToF-SIMS total (positive) ion image of particles in the pyrite/sphalerite/chalcopyrite mixture. Left: linear scale. Right: log scale.

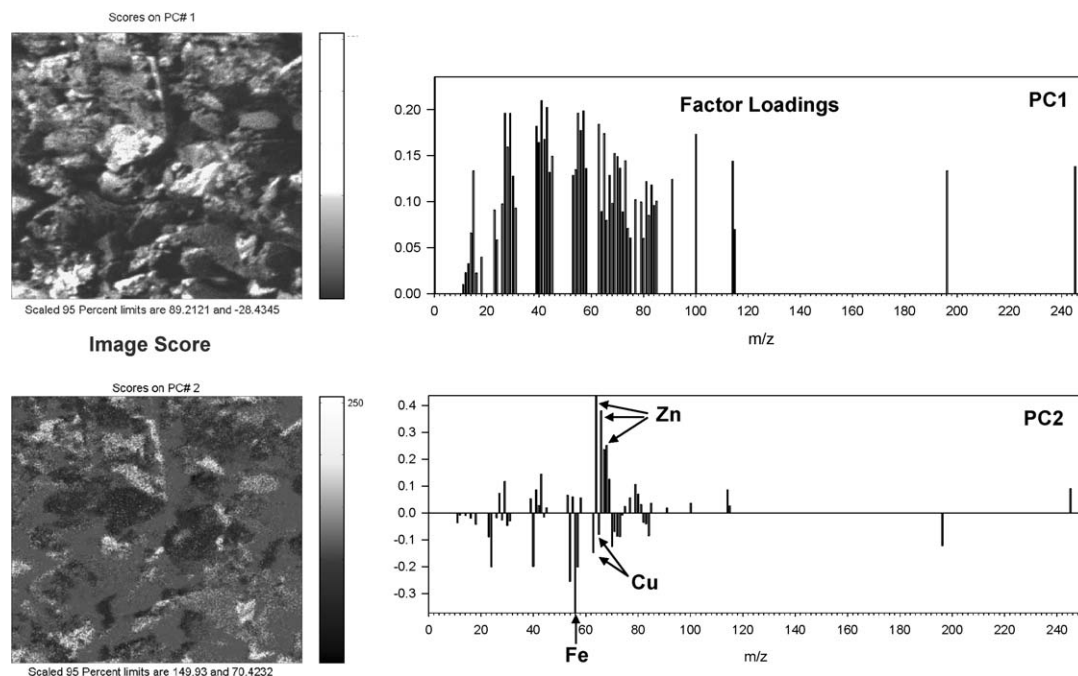


Fig. 5. Principal component image scores and factor loadings for the chalcopyrite/pyrite/sphalerite mixture (“autoscaled” data, positive ion ToF-SIMS image data). Images are  $100 \times 100 \mu\text{m}$ .

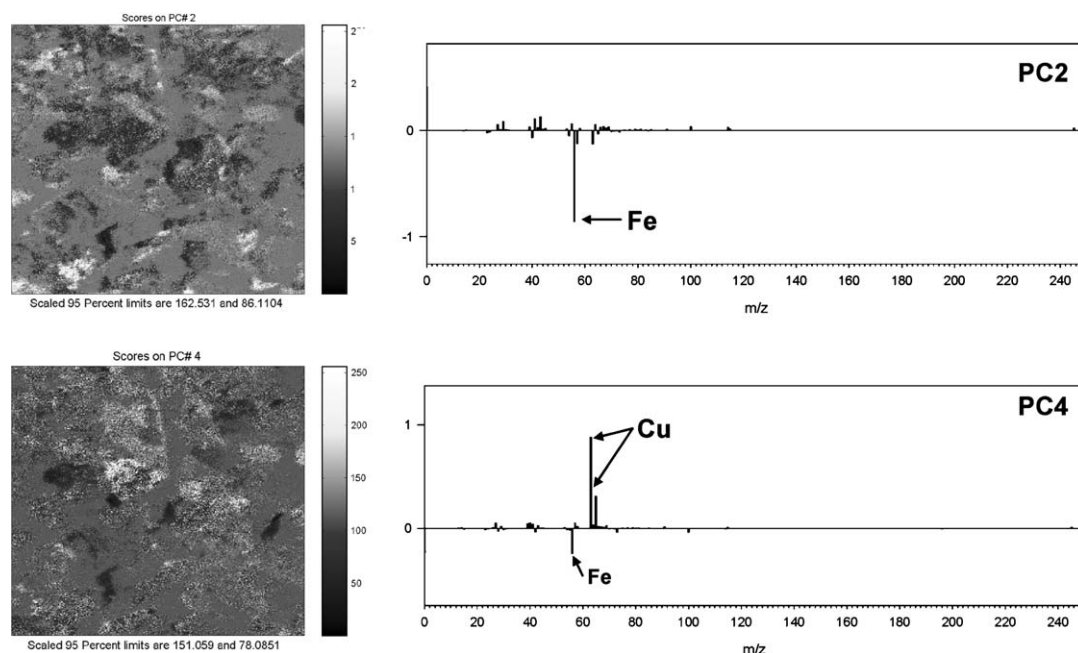


Fig. 6. Principal component image scores and factor loadings (PC2 and PC4 only) for the chalcopyrite/pyrite/sphalerite mixture (“mean centred” data, positive ion ToF-SIMS image data). Images are  $100 \times 100 \mu\text{m}$ .

negative loading for iron and is similar in spatial distribution to the dark areas of PC2 from the “autoscaled” data set in Fig. 5. PC4 in Fig. 6 has strong positive loadings for copper. Thus the bright areas in the images are rich in copper giving positive chalcopyrite identification and by elimination, pyrite. Using these two PC analyses the chalcopyrite, pyrite, sphalerite, gangue materials and back-

ground (indium) components can be fully identified. It is therefore possible to select ROIs for each mineral with increased precision.

From the PC analysis, new ROI's were mapped (Fig. 7), spectra collected and the information processed in the same manner as the previous single specie ion image analyses. The differentiation of pyrite from sphalerite is clearly illus-

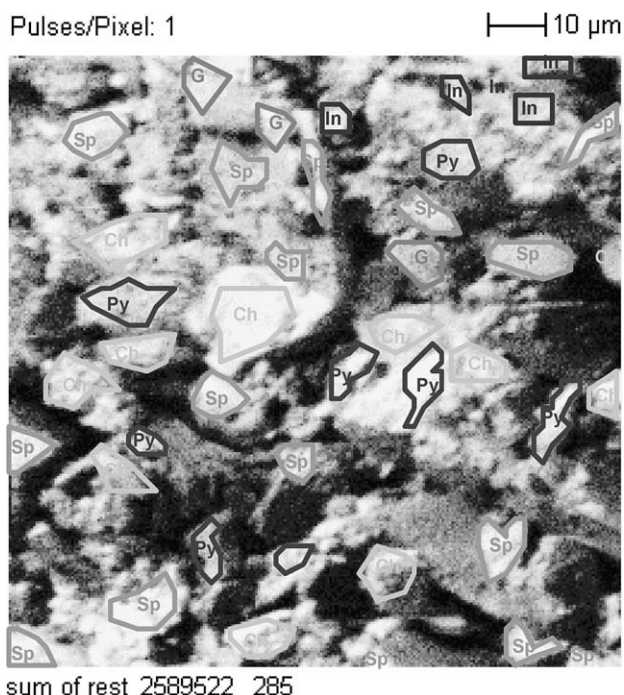


Fig. 7. PCA identification of mineral phases labelled: pyrite (Py); sphalerite (Sp); chalcopyrite (Ch); gangue materials (G), indium mounting material (In).

trated in the analyses of spectra collected from different ROIs (Fig. 8). The areas selected as pyrite contain appreciably more Fe than sphalerite; the Fe signal from sphalerite regions is consistent with a high-Fe sphalerite phase. Spectra for sphalerite grains are clearly Zn rich relative to pyrite; the Zn signal in the latter is likely superficial.

Importantly, using PCA phase identification, we now see a clear statistical separation of Cu distribution in favour of sphalerite (Fig. 8 left). The close agreement between the two copper isotopes provides confidence in the validity of the separation. This is also consistent with unwanted flotation of this phase in chalcopyrite circuits (Finkelstein, 1997). The transfer of copper ions from chalcopyrite dissolution to both pyrite (Smart, 1991) and sphalerite surfaces (Finkelstein, 1997) is confirmed by the surface analysis (Fig. 8 right). The new result is direct sta-

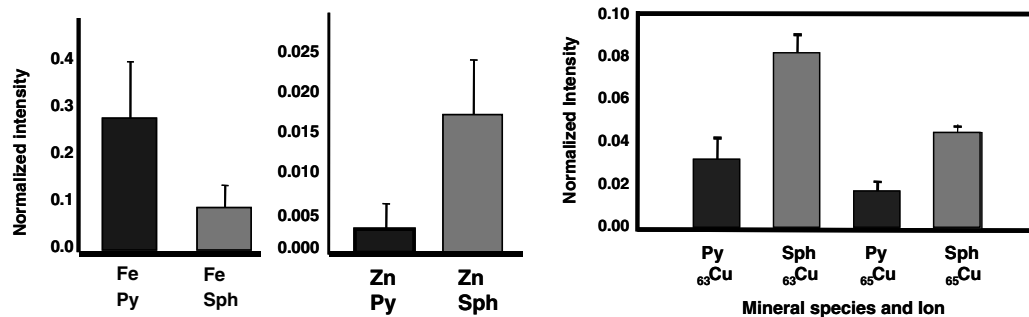


Fig. 8. PCA phase identification, pyrite from sphalerite. Left: note lower contributions from Zn on pyrite compared with Zn on sphalerite (cf. Fig. 4). Right: statistical analysis of Cu distribution between pyrite and sphalerite using the phase regions identified by PCA.

tistically-based evidence of preferential adsorption on sphalerite over pyrite in the same conditions and pulp solution.

### 3.2. Plant samples

The Inco Nickel–Copper Matte flotation process (Sprole et al., 1945; Tipman et al., 1976) separates chalcocite ( $\text{Cu}_2\text{S}$ , Cc) from heazlewoodite ( $\text{NiS}$ , Hz) using a diphenylguanidine (DPG) collector and frother. The separation becomes less selective as the minerals move through the circuit. Possible reasons suggested for this loss include:

- inadvertent activation of Hz by dissolved copper ions;
- depression of Cc by dissolved nickel ions;
- lack of selectivity of the diphenylguanidine (DPG) collector including slow formation of Ni–DPG complexes at Hz surfaces and; possible requirement of oxidation of Cc surfaces before effective DPG adsorption;
- depressant action of the calcium ions introduced as lime in the control of pH to 11–12 in this circuit.

We have used the same PCA methods to study concentrate and tail samples from the operating plant. The principal components gave excellent recognition of the two mineral phases with reliable statistics on the regions selected. Fig. 9 illustrates some of the results from this study. Direct evidence of Cu transfer from chalcocite to heazlewoodite on particles inadvertently collected into the concentrate is shown in Fig. 9(a). Evidence of Ni transfer from heazlewoodite to chalcocite in the tail samples is given in Fig. 9(b). The correspondence in this and subsequent figures between the isotopes of Cu(63,65) and Ni(58,60) again gives some confidence in the correlations.

The inadvertent flotation of Hz in the concentrate appears to be a result of Cu activation ( $\text{Cu}_{63} = 0.16$ ). There is also abundant Cu on Hz particles in the tails ( $\text{Cu}_{63} = 0.08$ ) but this is roughly half that in the concentrate. The Cu distribution between Cc and Hz particles in both concentrate and tails is the same within statistical 95% confidence intervals. The large statistical difference is in the Ni distribution where there is much ( $\sim 5\times$ ) more hydrophilic Ni(II) ions on Cc particles in the tail compared

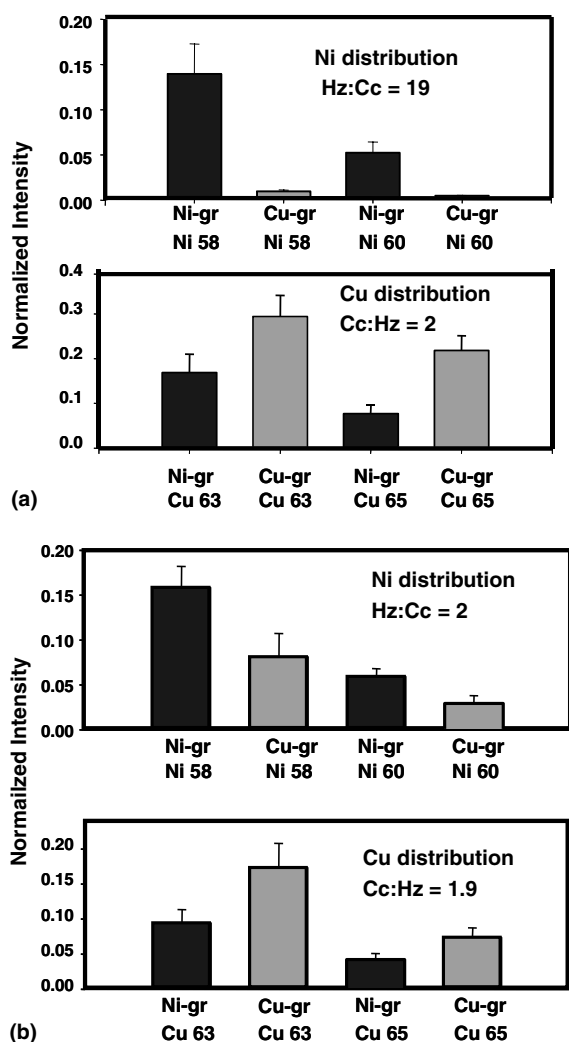


Fig. 9. (a) Matte Concentrator concentrate sample. PCA phase recognition with statistical analysis of phase regions for Ni and Cu transfer. Upper: note the clear separation of surface nickel between Hz and Cc. Lower: note the relatively high surface concentrations of Cu (both isotopes) on heazlewoodite (Ni-gr). (b) Matte Concentrator tails sample. PCA phase recognition with statistical analysis of phase regions for Ni and Cu transfer. Upper: note the loss of separation of surface nickel between Hz and Cc (cf. concentrate). Much higher surface concentrations on Cc in tails. Lower: note the still relatively high surface concentrations of Cu (both isotopes) on heazlewoodite (Ni-gr) in tails.

with the concentrate. Hence, Cc in tails appears to be the result of high depressant hydrophilic loadings rather than absence of hydrophobic CuDPG surface species (see Fig. 11). The exposure of Cu on Cc particles in the tails cf. concentrate is  $\sim 0.5$  corresponding to an increase in Ni exposure of  $\sim 7.5$ . Both Cu activation of Hz and Ni depression of Cc are clearly operating in this system.

The possible depressant action of Ca ions is not found to be selective. Fig. 10 shows that Ca is found on both Cc and Hz surfaces in concentrate and tails in statistically inseparable signals. Hence, Ca is adsorbed on all surfaces but is not discriminating between mineral particles of the same phase in concentrate and tails.

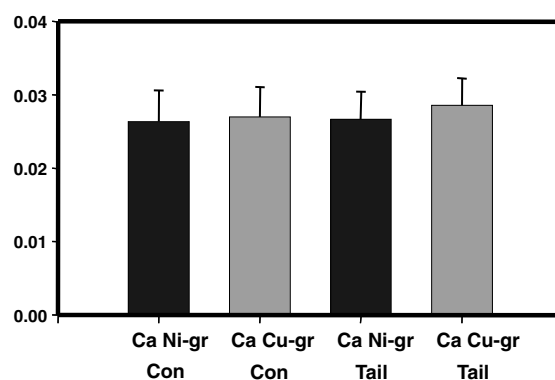


Fig. 10. Matte concentrator PCA phase recognition with statistical analysis of phase regions for Ca signals in concentrate and tails samples.

Mass signals for the Cu–DPG complex, represented in the mass 119 fragment, show higher ( $>1.8\times$ ) surface concentrations on Hz in the concentrate compared with the tail (Fig. 11). There is considerably more DPG ( $>4\times$ ) on Cc particles in concentrate than tails. In the tail samples there is no statistical difference in intensity of the DPG signals between Hz and Cc (Fig. 11). The reduced chalcocite hydrophobic/hydrophilic ratio is therefore related to the presence of Ni on the surface, with a consequent reduction in bubble attachment efficiency.

There is also evidence that DPG may selectively attach to hydroxylated Cu sites. There is considerably higher ( $>2\times$ ) CuOH signal on both Cc and Hz particles in the concentrate than in the tails although more CuO is measured on both minerals in tails than concentrate. This finding is supported by Pearson product moment correlations giving high correlation coefficients between CuOH and DPG (119) on Hz in concentrate (0.70) and tails (0.90) and for Cc in concentrate (0.96). The correlation coefficient for Cc in tails is lower (0.3) presumably due to the high surface concentrations of Ni ions.

The most time-consuming steps in this analysis are the post-ToF-SIMS and PCA marking out of the ROIs, the collection of the mass spectra from the pixels in each ROI and the spread sheet statistical analysis of the collected spectra. The PCA analysis has already identified correlations of other species with major elements in particular mineral phases. It may be possible to directly compare PCs identifying specific mineral phases between concentrate and tails as in Fig. 12 but this analysis requires validation against the ROI method. If this is successfully validated, this methodology would allow full diagnostic assessment of surface speciation control in a single day turn-around.

Fig. 12 does confirm the high correlation of DPG with Cu in concentrate as CuDPG fragments and, conversely, no correlation of DPG with Ni and NiOH in concentrate or tail. These results agree with the ROI analysis. It also points to high correlation of Fe with Ni in concentrate which may be as a lattice substituent in Hz. The correlations of CuOH, K and Ca with tails in high Cu areas do not appear to agree with Figs. 10 and 11 but the correlation



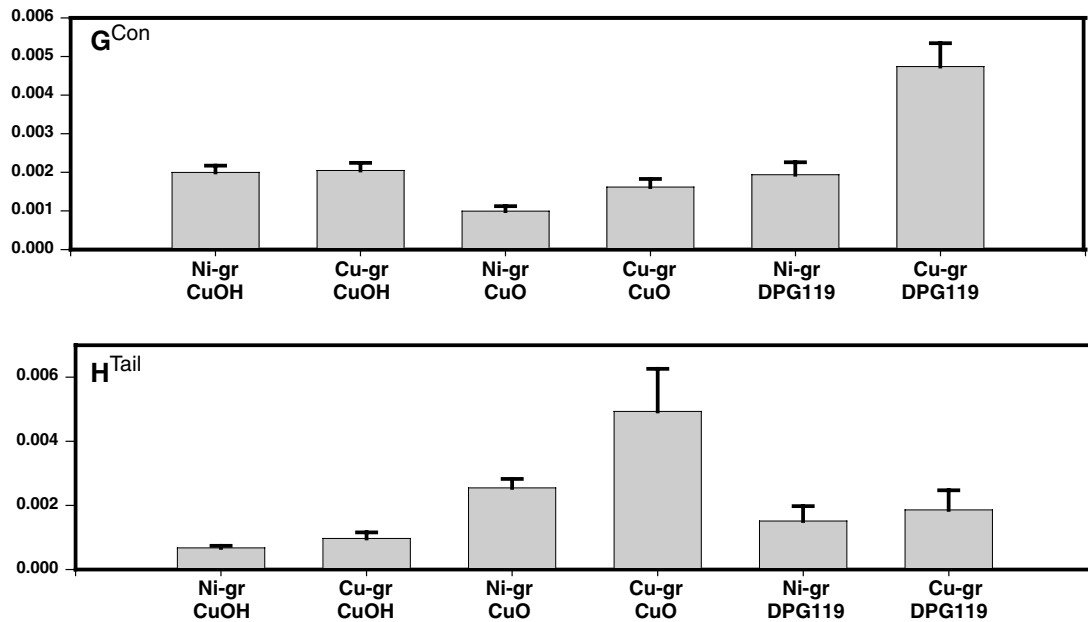


Fig. 11. Comparison of CuOH, CuO and DPG mass signals. G: Concentrate, high surface concentration of Cu–DPG complex on Hz (Ni–gr), H: Tail, no statistical difference in DPG between Cc (Cu–gr) and Hz (Ni–gr). Higher CuOH on concentrate.

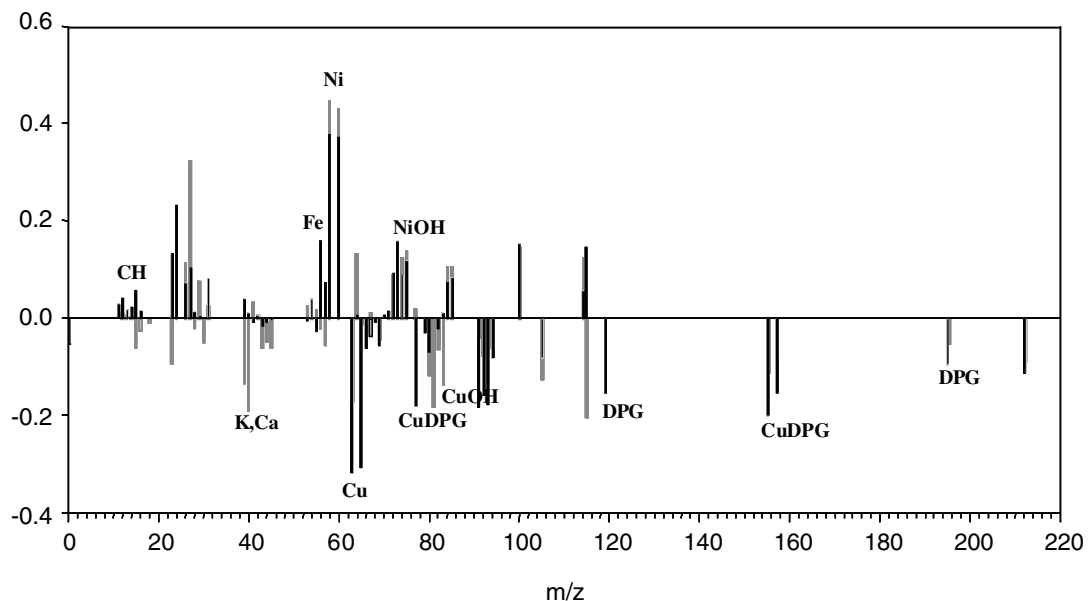


Fig. 12. Overlay of principal components (second) identifying Ni and Cu regions between concentrate (dark) and tails (light).

of PC2 in the tails with Cu is weak (particularly for the 63 isotope) probably again due to substantial coverage by precipitated  $\text{Ni}(\text{OH})_2$ . A more complete understanding of the PCA information may allow further processing and/or normalisation. This will be the next step in our work in progress.

#### 4. Conclusions

Diagnosis of the surface chemical factors playing a part in flotation separation of a valuable sulfide phase requires

measurement of activating species that are statistically different between mineral phases. Time of flight secondary ion mass spectrometry (ToF-SIMS) has been used to identify sufficient particles of a specific mineral phase for reliable statistics determining a mean value for each species with 95% confidence intervals.

For a chalcopyrite/pyrite/sphalerite mineral mixture conditioned at pH 9 for 20 min, transfer of Cu from chalcopyrite occurred via solution to the other two mineral surfaces. Analysis based on Fe and Zn images indicated no statistical difference in the copper intensities on pyrite

and sphalerite after this conditioning. Principal component analysis (PCA) is a better method of selecting mineral phases due to multi-variable recognition. The combination of auto-scaled and mean-centered principal components applied to this mineral mixture of pyrite, sphalerite and chalcopyrite, clearly separated the various mineral phases and enabled more reliable identification of statistical differences in copper intensities between the sphalerite and pyrite phases.

The method has been extended to samples from an operating flotation plant again with excellent phase recognition and diagnostic surface chemistry. Both copper and nickel ion transfer via solution have also been demonstrated in this study, the former relating to inadvertent activation of heazlewoodite and the latter to inadvertent depression of chalcocite. The methodology, with PCA phase recognition and statistical analysis, considerably extends the analytical basis of surface chemical control in flotation.

### Acknowledgements

This work is supported by a Canadian NSERC Discovery Grant to RStCS and by an exchange program between ACeSSS and Surface Science Western. We are particularly grateful to Prof. Stewart McIntyre (Director, SSW) for the latter arrangement. The assistance of Inco Sudbury with plant sampling (Mr. Jim Truskoski, Ms. Cassandra Valenius, Dr. Dan Legrand) and permission to publish the results (Dr. Peter Wells) has been central to this project and is much appreciated.

### References

- Biesinger, M.C., Paepegaey, P.-Y., McIntyre, N.S., Harbottle, R.R., Petersen, N.O., 2002. Principal component analysis of ToF-SIMS images of organic monolayers. *Anal. Chem.* 74, 5711–5716.
- Biesinger, M.C., Miller, D., Francis, J., Hart, B., Smart, R.St.C., 2004. Principal component analysis applied to surface chemistry in minerals flotation. In: Laskowski, J.S. (Ed.), *Particle Size Enlargement in Mineral Processing*, Proc. of the Fifth UBC–McGill Int. Conf. Fundamentals of Mineral Processing. Canadian Inst. Mining, Metallurgy and Petroleum. ISBN 1-894475-52-6, pp. 73–88.
- Finkelstein, N.P., 1997. The activation of sulfide minerals for flotation: a review. *Int. J. Miner. Process.* 52, 81–120.
- Gerson, A.R., Lange, A.G., Prince, K.P., Smart, R.St.C., 1999. The mechanism of copper activation of sphalerite. *Appl. Surf. Sci.* 137, 207–223.
- Hart, B., Biesinger, M., Smart, R.St.C., 2005. Improved statistical methods applied to surface chemistry in minerals flotation. In: Jameson, G. (Ed.), *Proc. Centenary of Flotation Symp.* Publ. AusIMM, Carlton, Victoria, Australia, pp. 457–464.
- Lascelles, D., Finch, J.A., 2002. Quantifying accidental activation I. Cu ion production. *Miner. Eng.* 15, 567–571.
- Mardia, K.V., Kent, J.T., Bibby, J.M., 1979. *Multivariate Analysis*. Academic Press, London, pp. 213–254.
- Massart, D.L., Vandeginste, B.G.M., Buydens, L.M.C., De Jong, S., Lewi, P.J., Smeyers-Verbeke, J., 1997. *Handbook of Chemometrics and Qualimetrics: Part A*. Elsevier, Amsterdam, pp. 519–556.
- Piantadosi, C., Jasieniak, M., Skinner, W.M., Smart, R.St.C., 2000. Statistical comparison of surface species in flotation concentrates and tails from ToF-SIMS evidence. *Miner. Eng.* 13, 1377–1394.
- Ralston, J., 1994. Bubble–particle capture. In: Castro, S., Alvarez, J. (Eds.), *Flotation II*, vol. 2. Publ. Andros Ltd., Chile, p. 1464.
- Smart, R.St.C., 1991. Surface layers in base metal sulphide flotation. *Miner. Eng.* 4, 891–909.
- Smart, R.St.C., Jasieniak, M., Piantadosi, C., Skinner, W.M., 2003a. Diagnostic surface analysis in sulfide flotation. In: J. Ralston, J.D. Miller, J. Rubio (eds.), *Flotation and flocculation: From fundamentals to applications*. ISBN 0-9581414-0-1, 28 July–2 August 2002, Hawaii. Publ. Ian Wark Research Institute, University of South Australia, 241–248.
- Smart, R.St.C., Amarantidis, J., Skinner, W.M., Prestidge, C.A., LaVannier, L., Grano, S.G., 2003b. Surface analytical studies of oxidation and collector adsorption in sulfide mineral flotation. In: Wandelt, K., Thurgate, S. (Eds.), *Solid–liquid interfaces*, Topics in Applied Physics, 85. Springer-Verlag, Berlin, pp. 3–60.
- Sproule, K., Harcourt, G.A., Rose, E.H., 1945. Froth Flotation of Nickel–Copper Matte, US Patent No. 2,432,465.
- Tipman, N.R., Agar, G.E., Pare, L., 1976. Flotation chemistry of the Inco Matte separation process. In: Fuerstenau, M.C. (Ed.), *Flotation*, A.M. Gaudin Memorial Volume, 1. Amer. Inst. Min. Metall. Petrol. Eng. Inc., pp. 528–548, Chapter 18.
- Weisener, C., Gerson, A.R., 2000. Cu(II) adsorption mechanism on Pyrite: an XAFS and XPS study. *Surf. Interf. Anal.* 30, 454–458.